



LIGO Laboratory / LIGO Scientific Collaboration

LIGO-T0900423-v3

Advanced LIGO

October 15, 2010

Transmission Monitor Quadrant Photodetector Design

Rich Abbott, Peter Fritschel

Distribution of this document:
LIGO Scientific Collaboration

This is an internal working note
of the LIGO Laboratory.

California Institute of Technology
LIGO Project – MS 18-34
1200 E. California Blvd.
Pasadena, CA 91125
Phone (626) 395-2129
Fax (626) 304-9834
E-mail: info@ligo.caltech.edu

Massachusetts Institute of Technology
LIGO Project – NW22-295
185 Albany St
Cambridge, MA 02139
Phone (617) 253-4824
Fax (617) 253-7014
E-mail: info@ligo.mit.edu

LIGO Hanford Observatory
P.O. Box 1970
Richland WA 99352
Phone 509-372-8106
Fax 509-372-8137

LIGO Livingston Observatory
P.O. Box 940
Livingston, LA 70754
Phone 225-686-3100
Fax 225-686-7189

<http://www.ligo.caltech.edu/>

1 Overview

The alignment control system for aLIGO uses the beams transmitted by the End Test Masses (ETMs) for sensing fluctuations of the arm cavity mode position, as described in T0900511, *Modeling of Alignment Sensing and Control for Advanced LIGO*. For each ETM transmitted beam, there will be two quadrant detectors, to sense both near-field and far-field motions and these detectors will be located within the ETM BSC vacuum chamber on the suspended Transmission Monitor platform (these will be called the TransMon Quads). In addition, two more quadrant detectors will be mounted on this platform to sense the position of the Arm Length Stabilization beam, which is a 532 nm beam injected into the arm from each end station (these will be called the ALS Quads). The two types of quad detectors will use similar mounting and electronics, though the actual photodiodes are different.

For both types of detectors, only the quad diode element will be mounted in the vacuum chamber on the TransMon platform. The amplifier trans-impedance circuitry and associated whitening filters will be located outside the vacuum envelope. A sense-wire type noise cancellation scheme will be employed in a manner identical to the successful ELIGO OMC QPD (see Appendix A). This document contains the design of the trans-impedance amplifiers and whitening filters, details of the photodiodes and diode mounts, and results from prototype electronics.

2 Photodiodes

For the 1064 nm beam detection, we need to detect 50 mW of light at full power operation of the interferometer. We use an InGaAs quad-diode, specifically the OSI Q3000; this is the same diode that will be used in the wavefront sensors (WFSs) and that has been used in eLIGO for in-vacuum detection of the AS port beam. The diode is in a TO-5 package; the window will be removed (by us), and the resulting package is exposed to the vacuum, so vacuum compatibility is an issue. The vendor does use epoxy to bond the semiconductor to the can, though they have not been willing to tell us what type is used. These quad diodes are currently being vacuum tested/qualified by LIGO. They have passed the RGA scanning test, and are currently in a contamination test cavity setup.

For the 532 nm beams, InGaAs gives essentially no response, so we need to use a silicon photodiode instead. Our leading candidate is the Perkin-Elmer C30845E. Again there is epoxy used to bond the silicon to the package, but PE is more forthcoming: it uses EPO-TEK H20E from Epoxy Technologies (this is a NASA approved low outgassing adhesive). These diodes will be submitted to the LIGO vacuum qualification queue. These diodes will be designed to detect a power level of 0.1—1 mW.

<i>Vendor</i>	<i>Model</i>	<i>Material</i>	<i>Size</i>	<i>Response</i>
OSI	Q3000	InGaAs	3 mm diam.	0.8 A/W @1064 nm
Perkin-Elmer	C30845E	Silicon	8 mm diam.	0.3 A/W @ 532 nm

Biasing. Both types of photodiodes will be operated in photoconductive mode with a small reverse bias. Since low capacitance is not important, the bias is kept small to limit power dissipation. The InGaAs diodes will be biased at 1 V, and the silicon diodes at around 5 V.

3 Photodiode Mounts

Figure 1 and 2 show the back and front respectively of the proposed mounting scheme for the in-vacuum quad diode elements. This mounting scheme worked well for the eLIGO QPDs. Conductive cooling through the thick metal post will suffice to keep the diode element cool during foreseen operating conditions especially due to the low bias voltages for this design. The maximum power dissipation in the InGaAs quads is 50 mW optical plus $(1V * 40 mA)$ electrical, or about 100mW total. For the silicon diodes, it is 1 mW optical plus $(5V * 0.3 mA)$ electrical, or about 3mW total.

Figure 1

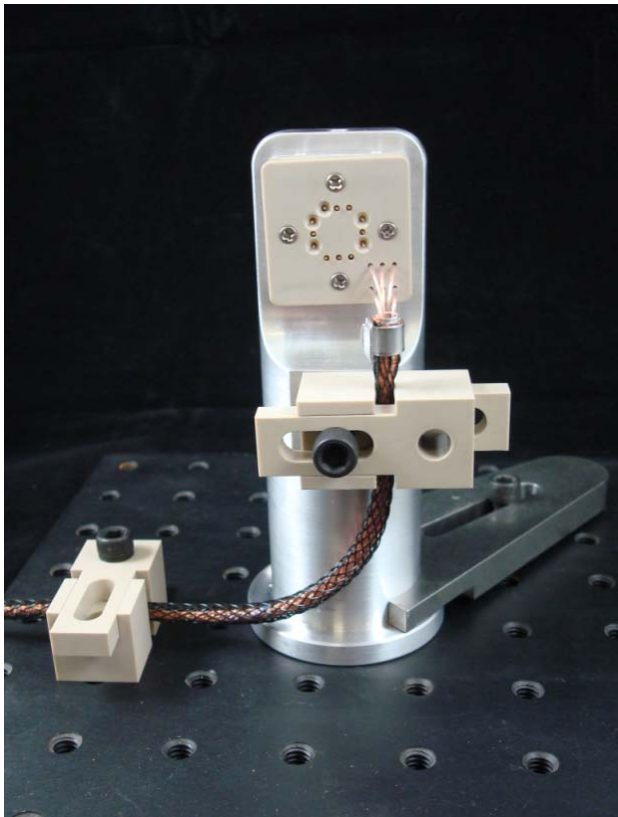
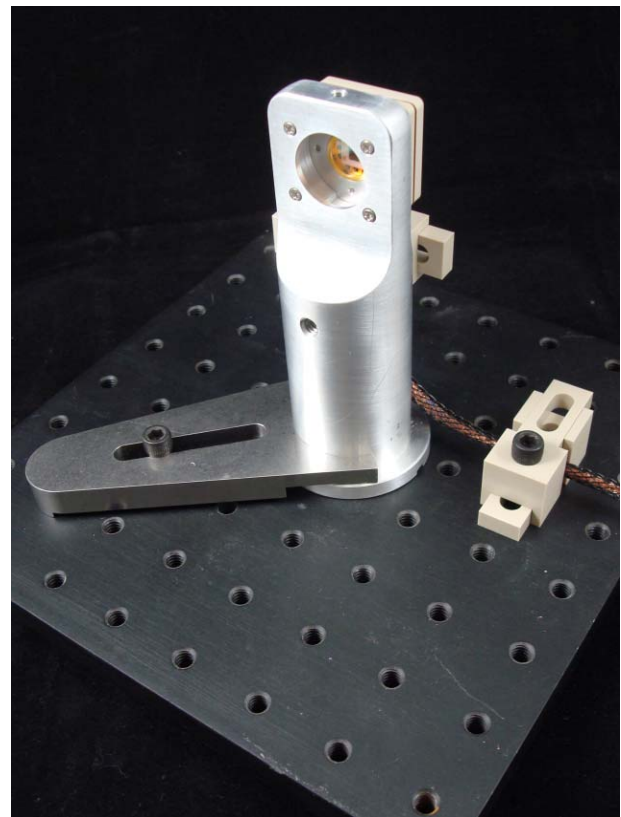


Figure 2



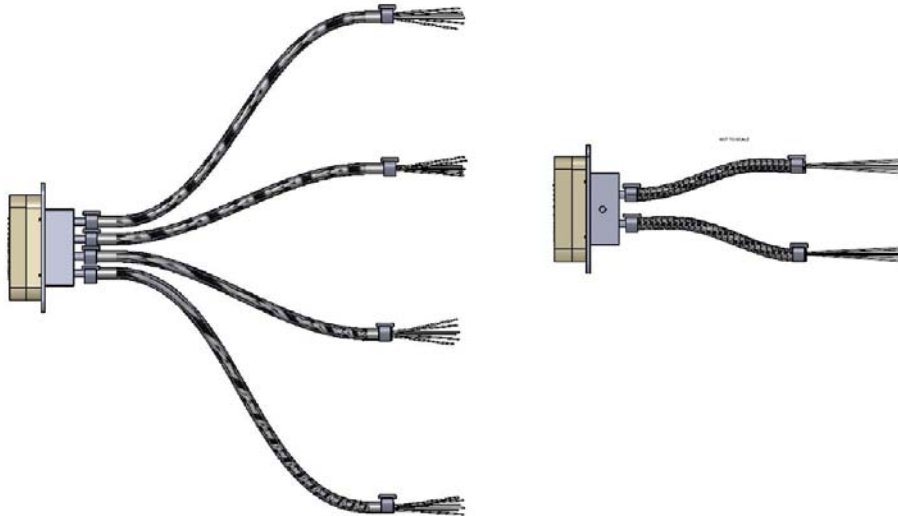
The basic building block for in-vacuum cabling is shown in Figure 3 and consists of a 13 foot long, female, 25 pin D-sub cable.

Figure 3



The 13 foot cable bridges between the vacuum flange and an application specific termination inside the vacuum system. For the Transmission Monitor, the choice of termination depends on the number of Transmission Monitors that are collocated in a given area. Figure 3 shows the two styles of in-vacuum cabling that will be used for the quad detectors. For a given application, the user has the choice of two or four QPDs per main 25 pin D-sub in-vacuum cable. The terminal end that mates to the QPD is as shown in figure 1, and can be of arbitrary length.

Figure 4



4 Transimpedance Amplifier

4.1 Readout requirements

The alignment control system requires the TransMon Quads to give shot-noise limited signals at frequencies above 10 Hz. At full interferometer input power (125 W), the TransMon optics will be arranged to give 50 mW on each TransMon Quad, which is the maximum power we are confident the photodiodes can operate at continuously. We may choose to initially set up the TransMon optics with a greater transmission to the quads, so that the 50 mW level is reached at a lower input power. In any case, the readout is designed so that electronics noise is at least a factor of 4 below shot-noise with 50 mW on the photodiode. This means that shot-noise will dominate the output over approximately a factor of 10 of the input power range. Furthermore, since the readout amplifier is external to the vacuum, better signal-to-noise at the low power end can always be achieved by changing the transimpedance value in the amplifier.

4.2 Amplifier design

The 4 identical channels of the readout circuitry use a true current-to-voltage (I to V) converter topology with negligible input impedance at audio frequencies. A single stage of whitening is included consisting of: DC gain of 1, one zero and one pole for a quasi-high-pass topology. This level of whitening is sufficient to ensure all signals down to the noise limit of the detector are transmitted at a level of 100nV/rtHz or larger at frequencies of ~ 0.5 Hz and above. A fully differential output driver stage is used to transmit the signal from the photodetector.

Since the photodetector is located in the vacuum system, with several meters of cabling between it and the front end amp, a sense wire is used to cancel the noise picked up on the wiring as the photocurrent is transported to the transimpedance amplifier. This was the technique used in the eLIGO OMC. This sense channel does add some additional electronics noise on each diode channel; however, since this sense channel noise is the same in each diode channel it is subtracted out of the actual alignment signals produced by the quad detector (it does remain in the sum channel).

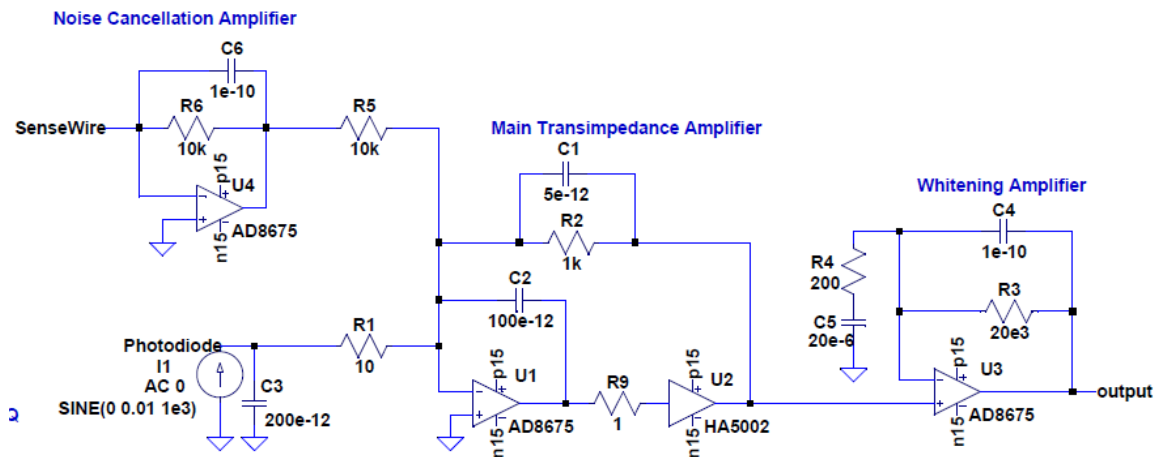
4.3 Amplifier specifications

- 1.1. Quiescent DC Current - + 102mA, -82mA as measured on the prototype circuit with 3.81VDC photodiode bias.
- 1.2. Detector noise is to be limited by shot noise for currents in excess of 1mA photocurrent
- 1.3. DC Supplies - +18VDC, -18VDC
- 1.4. Transimpedance – 1000 ohms (not including the differential driver gain)
- 1.5. Full Scale Photocurrent (per segment) – 15mA (produces 10VDC)
- 1.6. Maximum Steady-state Optical (total) – 100mW
- 1.7. Interface Connector – One 25 pin D-Sub.

4.4 Design Details

As seen in Figure 3, U1 and U2 form a transimpedance stage. The HA5002 is a no-frills, but reliable buffer that's easily capable of doing the job, and above all, is available. The choice of U1 results from a survey of available operational amplifiers, and produces the lowest combination of voltage and current noise for the operating transimpedance (667 ohms). There is nothing to preclude the choice of other amplifiers here, if other transimpedances were desirable. The current source and C3 represent a simplified model of one segment of the Q3000 photodiode. C3 has a 100 ohm series resistance internally included in its model. U3 forms a whitening stage yielding: a DC gain of one, zero at 0.4Hz, pole at 40Hz, and a Pole at 80 kHz. An additional zero results from C4 and R4, although this zero is swamped by the bandwidth of U3.

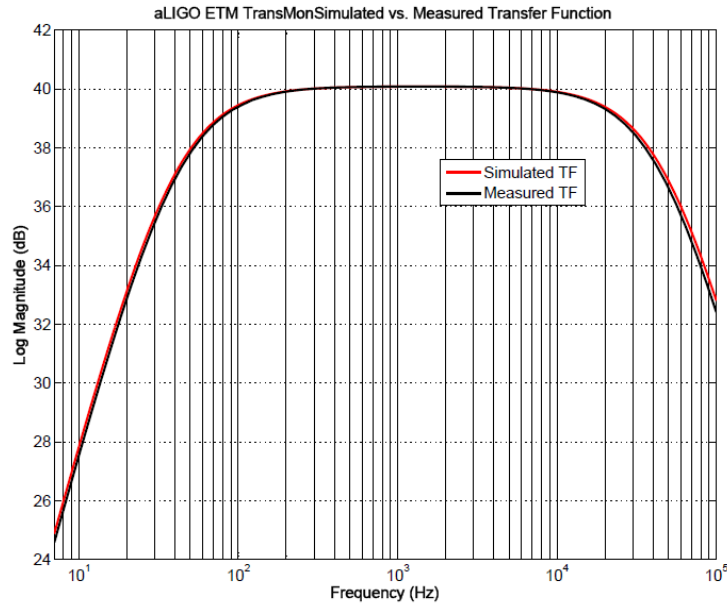
Figure 5



4.5 Transfer Function

Figure 4 shows an overlay of the simulated and measured transfer function. In order to make the measurement simple, a 1k resistor was tacked onto the input to U1. The result of this is to divide the total gain by 1000 as reflected in the annotation. The true gain is 60dB higher than plotted at the single ended output depicted in figure 1. An additional 6dB of gain will be present (not shown in figure 2) if one includes the differential driver gain.

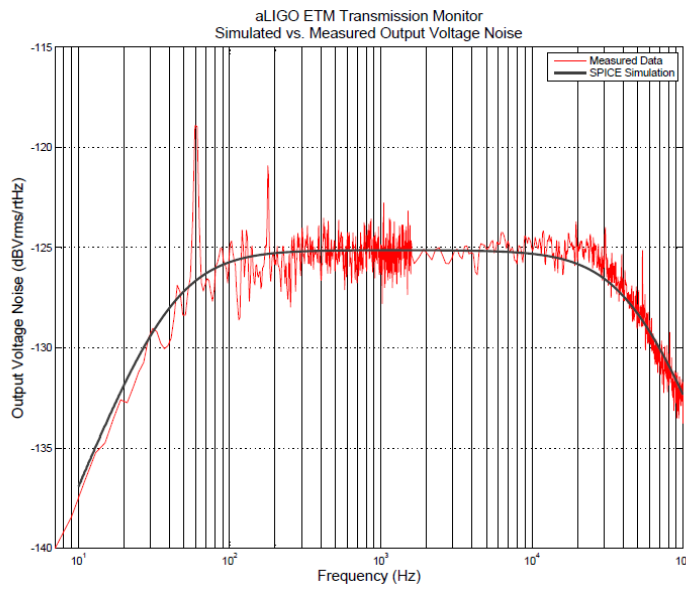
Figure 4 Transfer function of the transimpedance amplifier shown in Fig 3.



4.6 Output Noise Plot

Figure 5 shows an overlay of the simulated vs. measured output referred noise. The photodetector was biased at 3.81VDC, and shielded from stray light.

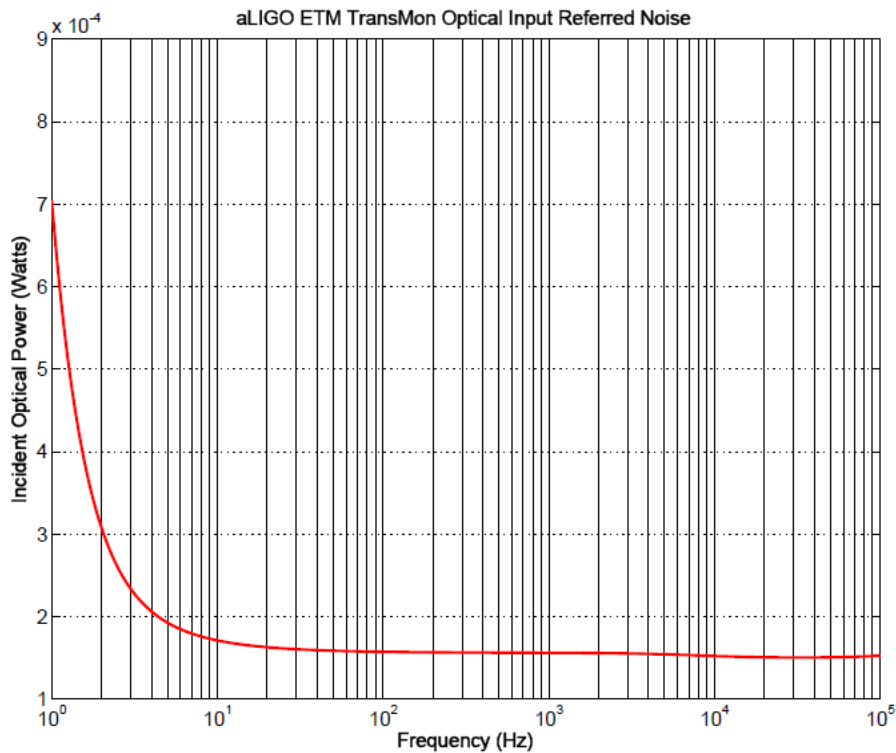
Figure 5. Output noise of the transimpedance amplifier shown in Fig. 3



4.7 Input Referred Optical Noise

Trusting the results of the output noise plot in figure 5, a plot is shown in figure 6 depicting the input referred optical power for 1064nm light incident on a single segment of a four-segment photodiode of 95% quantum efficiency. This curve represents a unity ratio of electronics noise to shot noise for the photodetector circuit. It answers the question; what is the minimum optical power for which a single segment of the QPD is shot noise limited?

Figure 6



To go from an electrical input referred noise in units of $A/\sqrt{\text{Hz}}$ to watts as shown in this plot, the following transformations are applied:

$$P = i_n^2 / (2 * e * 0.81), \text{ where:}$$

P = the incident optical power shown in the plot

i_n = the input referred current noise spectral density

e = electron charge

0.81 = A/W response at 1064nm, 95%QE conversion factor for the photodiode

4.8 Pitch and Yaw Noise vs. Sum Noise

Referring to the schematic of a single segment of the detector as shown in figure 3, it is worthy of note that in the four channel quadrant detector electronics, the additional electrical noise injected by the induced noise cancellation amplifier is applied in common mode to each channel. This additional electrical noise is present in the SUM channel, but is subtracted in the calculation of PITCH and YAW. Figure 7 shows curves for the incident optical power (1064 nm, 95%QE) in watts that will produce a shot noise signal equal to the electronics noise for an SNR of one. In the simulation of the PITCH readout, an optical input is divided among the four quadrants; the top two segments are driven as a pair differentially with respect to the bottom two segments to produce PITCH motion. YAW is identical to PITCH.

Figure 7

